Employing Ternary Fission as a Probe of Low Density Nuclear Matter

J. B. Natowitz [1], H. Pais [2], G. Röpke [3], J. Gauthier [1], K. Hagel [1], M. Barbui [1], and R. Wada [1]

[1] Cyclotron Institute, Texas A&M University, College Station, Texas 77843, USA
[2] CFisUC, Department of Physics, University of Coimbra, 3004-516 Coimbra, Portugal.
[3] University of Rostock, FB Physik, 18059 Rostock, Germany

–

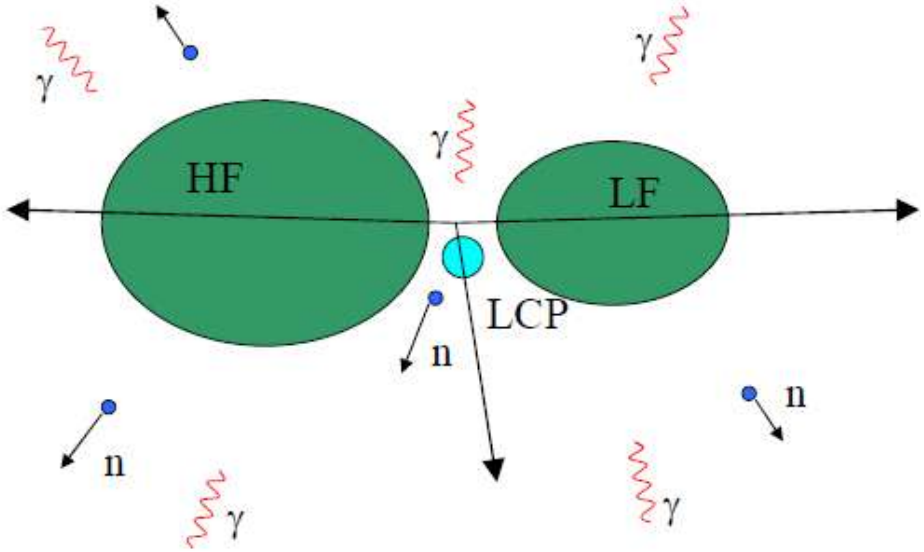

CYCLOTRON INSTITUTE
Texas A&M University

This Work is Part of a Larger, Ongoing Effort to Explore the Nuclear and Astrophysical Equations of State –

Establish relevance of laboratory experiments to simulations of the properties of low density surfaces in supernovae and binary mergers and to nucleosynthesis in neutrino driven winds

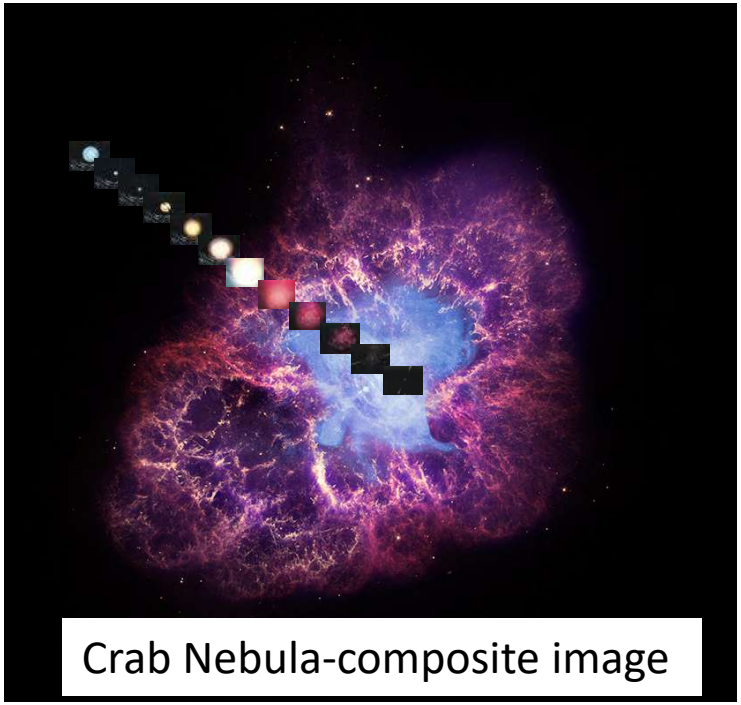

Crab Nebula-composite image

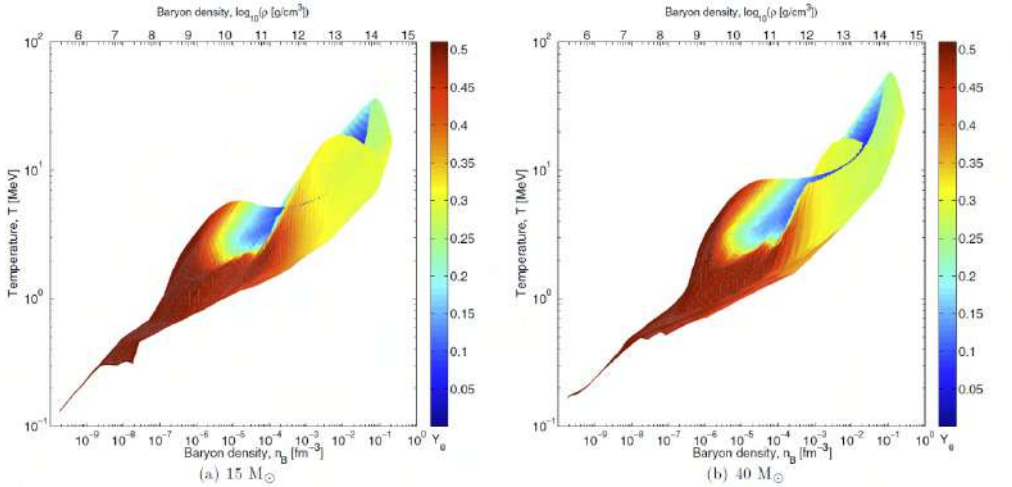

Figure 1. Phase space covered in core-collapse supernova simulations at the example of two progenitor models from Woosley & Weaver (1995), both using the pure hadronic EoS from Shen et al. (1998). The white background corresponds to densities and temperatures which are not obtained, where the colored domain belongs to densities and temperatures which are obtained. Color scale is the electron fraction which ranges from neutron matter (blue) $Y_e = 0$ to symmetric matter (red) $Y_e \simeq 0.5$.

(Animations and a color version of this figure is available in the online journal.)

CYCLOTRON INSTITUTE
Texas A&M University

Recent Focus on Cluster Formation at Low Density and Implications for Sites of Nucleosynthesis

K.Sumiyoshi et al., Astrophys.J. **629**, 922 (2005)

Density. electron fraction, and temperature profileof a 15 solar mass supernova at 150 ms after core bounce --as function of the radius.

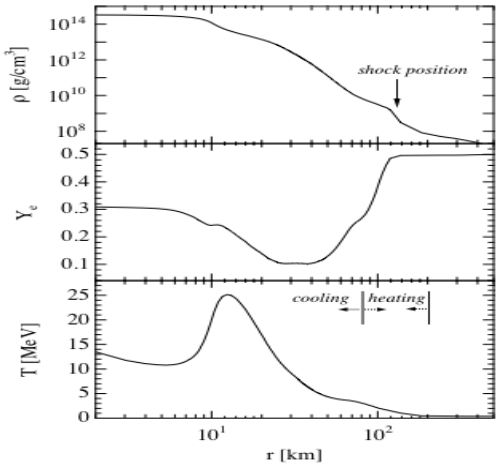

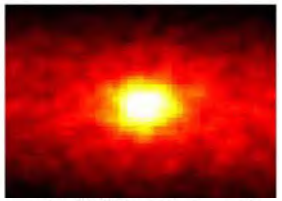

[C.J. Horowitz](), [A. Schwenk]()
ArXiv nucl-th/0507033

- Conditions at neutrinosphere:
  - Temperature ~ 4 MeV crudely observed with 20 SN1987a events.
  - **Density at last ν interactions**
  - $\rho \sim 10^{11}$ g/cm^3 [~10^{-4} fm^{-3}]

Similar temperatures and densities at neutrino surface in mergers of neutron stars and black holes

K.Sumiyoshi, G. Roepke PRC 77, 055804 (2008)

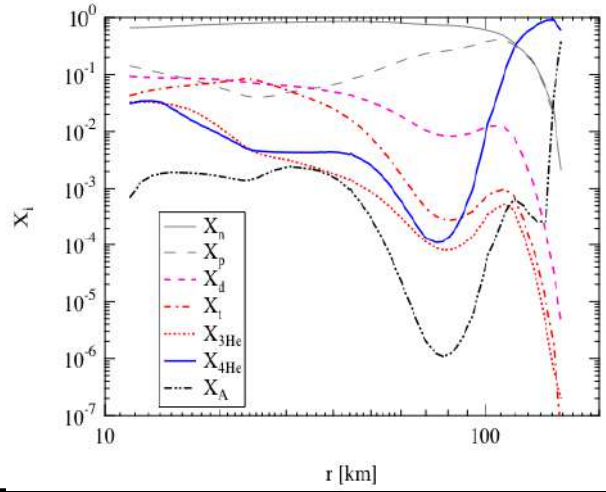

THE ASTROPHYSICAL JOURNAL, 745:170 (12pp), 2012 February 1 doi:10.1088/0004-637X/745/2/170

NEUTRINO SPECTRA FROM ACCRETION DISKS: NEUTRINO GENERAL RELATIVISTIC EFFECTS AND THE CONSEQUENCES FOR NUCLEOSYNTHESIS

O. L. CABALLERO[1,2], G. C. MCLAUGHLIN[1], AND R. SURMAN[3]
[1] Department of Physics, North Carolina State University, Raleigh, NC 27695, USA; lcaballe@uw.edu, olcaball@ncsu.edu, gail_mclaughlin@ncsu.edu
[2] Institute for Nuclear Theory, Seattle, WA 98195, USA
[3] Department of Physics and Astronomy, Union College, Schenectady, NY 12308, USA; surmanr@union.edu
Received 2011 May 31; accepted 2011 December 9; published 2012 January 16

ABSTRACT

Black hole (BH) accretion disks have been proposed as good candidates for a range of interesting nucleosynthesis, including the *r*-process. The presence of the BH influences the neutrino fluxes and affects the nucleosynthesis resulting from the interaction of the emitted neutrinos and hot outflowing material ejected from the disk. We study the impact of general relativistic effects on the neutrinos emitted from BH accretion disks. We present abundances obtained by considering null geodesics and energy shifts for two different disk models. We find that both the bending of the neutrino trajectories and the energy shifts have important consequences for the nucleosynthetic outcome.

CLUSTER FORMATION Influences neutrino flux,heating, nucleosynthesis

CYCLOTRON INSTITUTE
Texas A&M University

Nuclear Equation of State

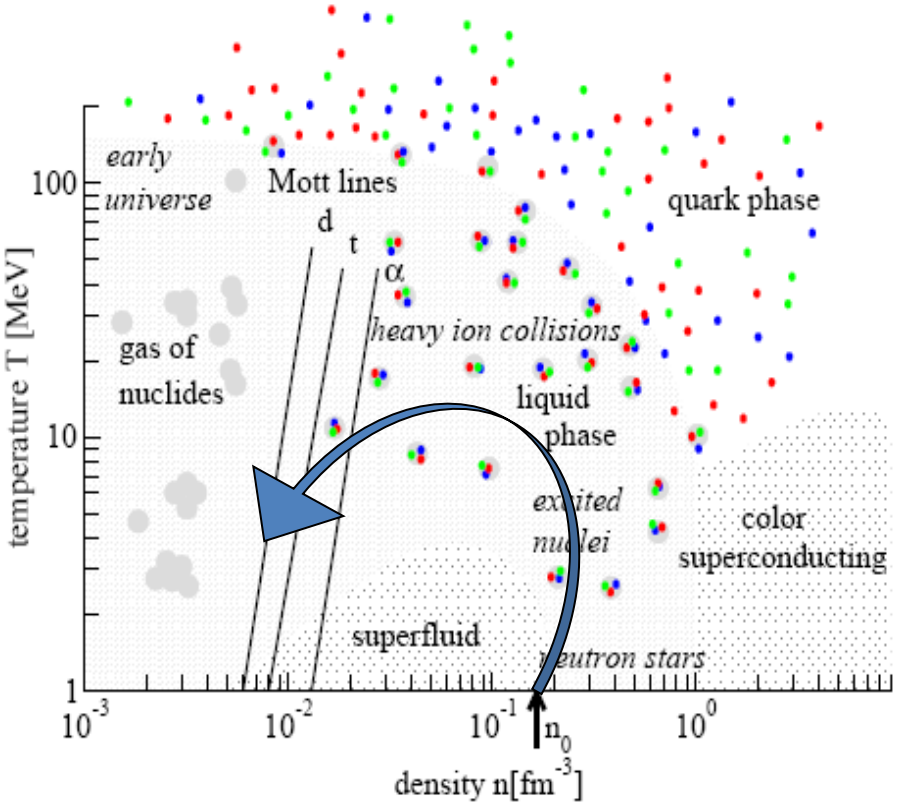

Employ near- Fermi energy nuclear collisions to probe low to medium temperature nuclear matter, primarily at sub-nuclear densities

Velocity Plots

Light Charged Particles- Most Violent Collisions

Experiments
47A MeV Projectiles

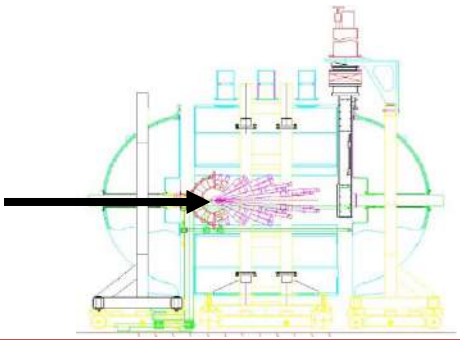

NIMROD- ISiS **4 Pi Charged Particles - 4 Pi Neutrons**

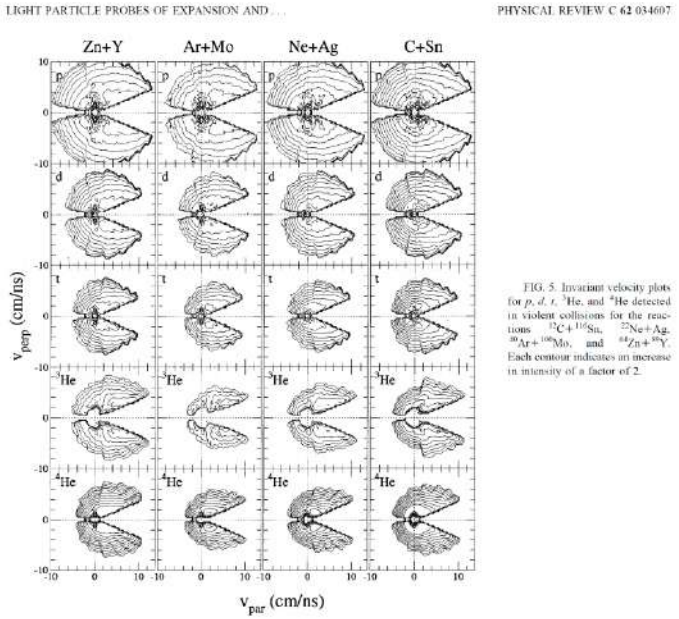

FIG. 5. Invariant velocity plots for p, d, t, ^{3}He, and ^{4}He detected in violent collisions for the reactions ^{12}C+^{116}Sn, ^{22}Ne+Ag, ^{36}Ar+^{106}Mo, and ^{64}Zn+^{89}Y. Each contour indicates an increase in intensity of a factor of 2.

From Fitting

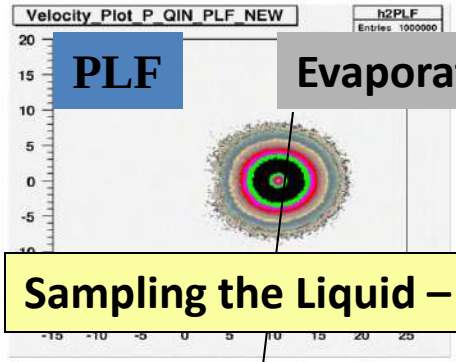

PLF **Evaporation-like**

Sampling the Liquid – late emission

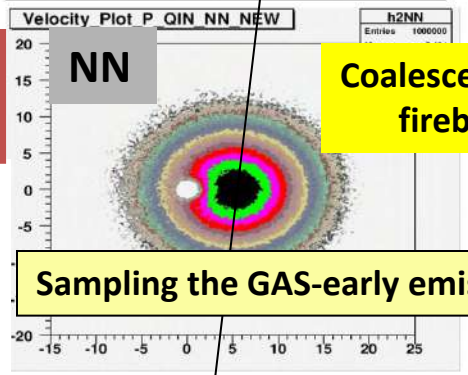

NN **Coalescence-like fireball**

Sampling the GAS-early emission faster particles

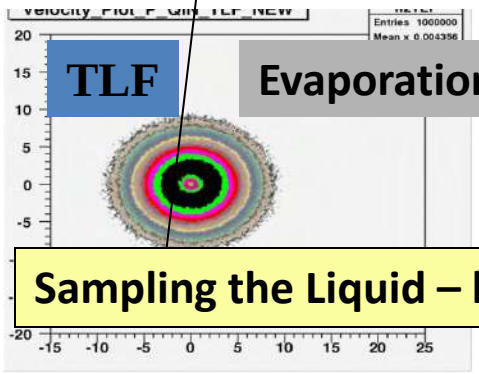

TLF **Evaporation-like**

Sampling the Liquid – late emission

Velocity Plot Protons
$^{40}Ar+^{124}Sn$
Thesis L-J Qin

Sum of Source Fits

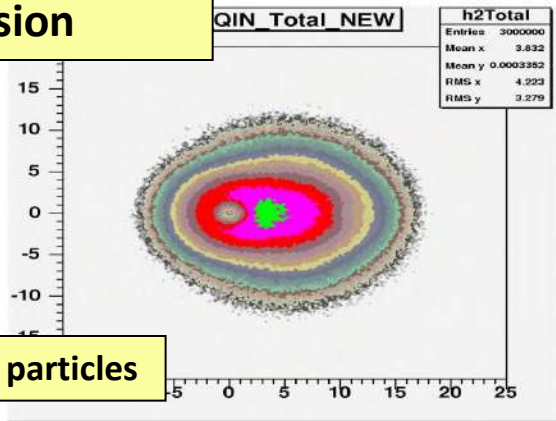

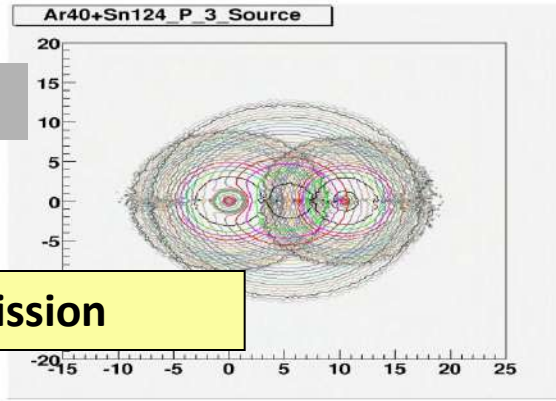

TEXAS A&M UNIVERSITY

Supernova

Mass: 4.6 ± 1.8 $M_{\odot}$. (~9.2×10^{30}kg)

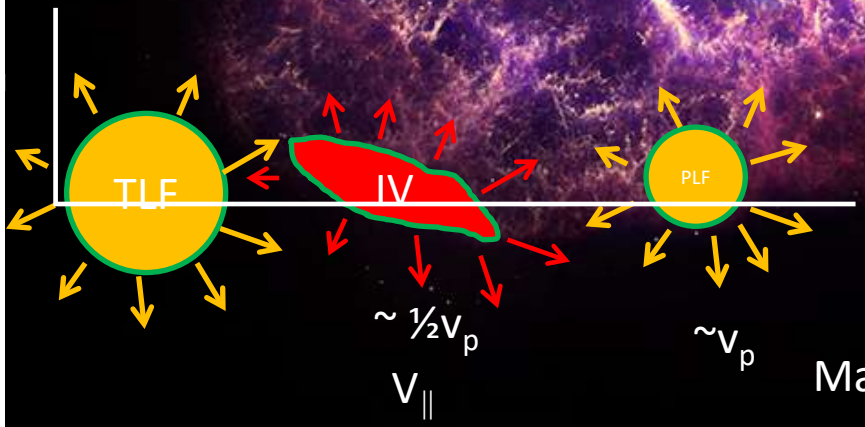

IV Source femtonova

Mass: 20-30 amu (~3.3×10^{-26} kg)

Analysis Based upon Thermal Coalescence Model Approach

$$\frac{d^2N(Z,N,E_A)}{dE_A d\Omega} = R_{np}^N \frac{A^{-1}}{N!Z!}\left[\frac{\frac{4}{3}\pi P_0^3}{[2m^3(E-E_c)]^{1/2}}\right]^{A-1} \times \left[\frac{d^2N(1,0,E)}{dEd\Omega}\right]^A. \quad (1)$$

$$V = \left[\frac{Z!N!A^3}{2^A}(2S+1)e^{E_0/T}\right]^{\frac{1}{A-1}} \frac{3h^3}{4\pi P_0^3}, \quad (2)$$

where E_0 is the binding energy of the cluster, S is the spin of the emitted cluster and T is the temperature of the system.

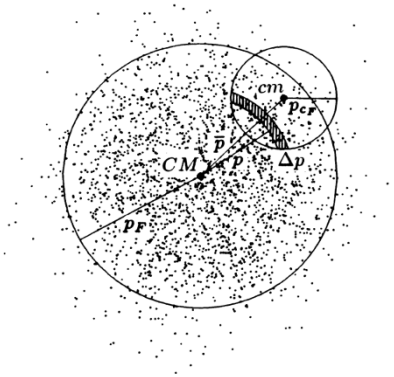

FIG. 2. Fermi spheres, in momentum space, of the composite nucleus and the cluster *c*.

L. P. Csernai and J. I. Kapusta, Phys. Rep. **131**, 223 (1986).
A. Z. Mekjian, Phys. Rev. C **17**, 1051 (1978); Phys. Rev. Lett. **38**, 640 (1977); Phys. Lett. **89B**, 177 (1980).
H. Sato and K. Yazaki, Phys. Lett. **98B**, 153 (1981).
T. C. Awes, G. Poggi, C. K. Gelbke, B. B. Back, B. G. Glagola, H. Breuer, and V. E. Viola, Jr., Phys. Rev. C **24**, 89 (1981).
K. Hagel et al.,Phys. Rev. C 62, 034607 (2000)

Temperatures and Densities

47 MeV/u ^{40}Ar + ^{112}Sn

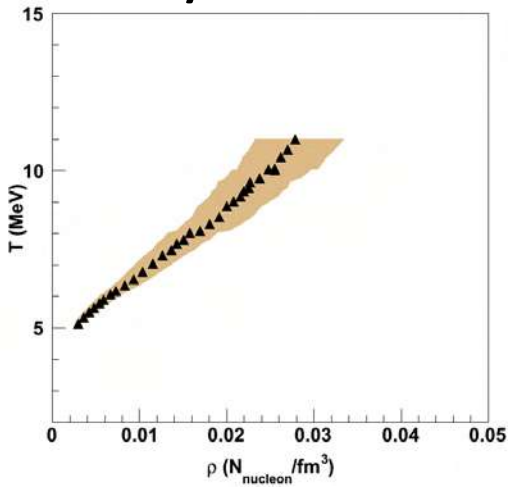

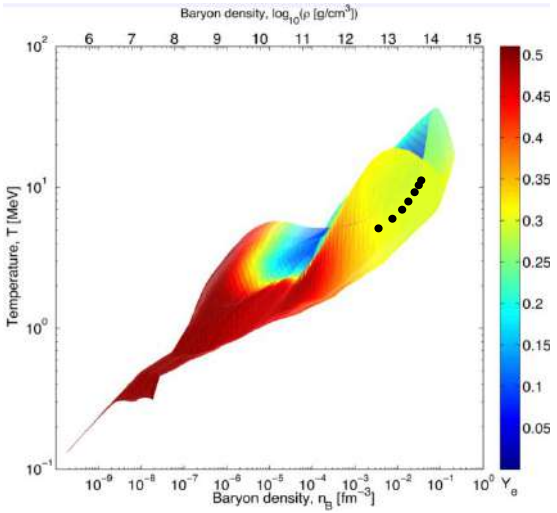

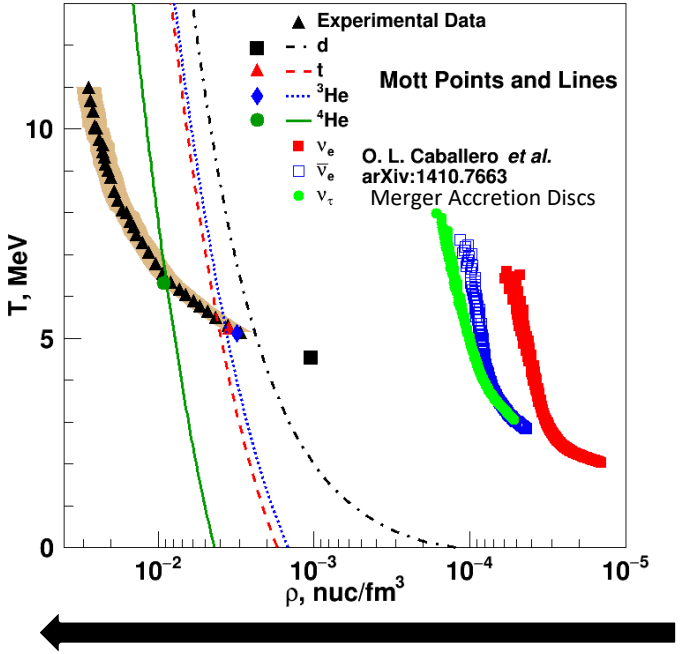

Data From

PRL 108, 172701 (2012).

PRL **108**, 062702 (2012).

Cyclotron Institute
Texas A&M University

COMPOSITION- CHEMICAL REACTION QUOTIENTS AND EQUILIBRIUM CONSTANTS

The reaction quotient, Q, of a chemical reaction at any time,t is

$$\alpha A + \beta B... \rightleftharpoons \rho R + \sigma S... \qquad Q = \frac{\{R\}^{\rho}\{S\}^{\sigma}...}{\{A\}^{\alpha}\{B\}^{\beta}...}$$

The equilibrium constant of a chemical reaction is the value of the reaction quotient when the reaction has reached equilibrium.

For a general chemical equilibriumthe thermodynamic equilibrium constant can be defined such that, at equilibrium,[1]

$$K^{\ominus} = \frac{\{R\}^{\rho}\{S\}^{\sigma}...}{\{A\}^{\alpha}\{B\}^{\beta}...}$$

where curly brackets denote the thermodynamic activities** of the chemical species..

An equilibrium constant value is independent of the analytical concentrations of the reactant and product species in a mixture, but depends on temperature and on ionic strength. Known equilibrium constant values can be used to determine the composition of a system at equilibrium.

The equilibrium constant is related to the standard Gibbs free energy change for the reaction.

$$\Delta G^{\ominus} = -RT \ln K^{\ominus}$$

If deviations from ideal behavior are neglected, the activities of solutes may be replaced by concentrations, [*A*], and the activity quotient becomes a concentration quotient, K_c.

$$K_c = \frac{[R]^{\rho}[S]^{\sigma}...}{[A]^{\alpha}[B]^{\beta}...}$$

K_c is defined in an equivalent way to the thermodynamic equilibrium constant but with concentrations of reactants and products instead of

** In chemical thermodynamics, **activity**) is a measure of the "effective concentration" of a species in a mixture. The species' chemical potential depends on the activity Activity depends on temperature, pressure and composition of the mixture, among other things. The difference between activity and other measures of composition arises because molecules in non-ideal gases or solutions interact with each other, either to attract or to repel each other.

Equilibrium constants for α-particles

PRL **108** (2012) 172701.

$$K_c(A,Z) = \frac{\rho(A,Z)}{\rho_p^Z \rho_n^{(A-Z)}}$$

- Many tests of EOS are done using mass fractions and various calculations include various different competing species.
- If any relevant species are not included, mass fractions are not accurate.
- Equilibrium constants are more robust than mass fractions.
- Differences in the equilibrium constants may offer the possibility to study deviations from ideality-interactions between species
- Models converge toward ideality at lowest densities.

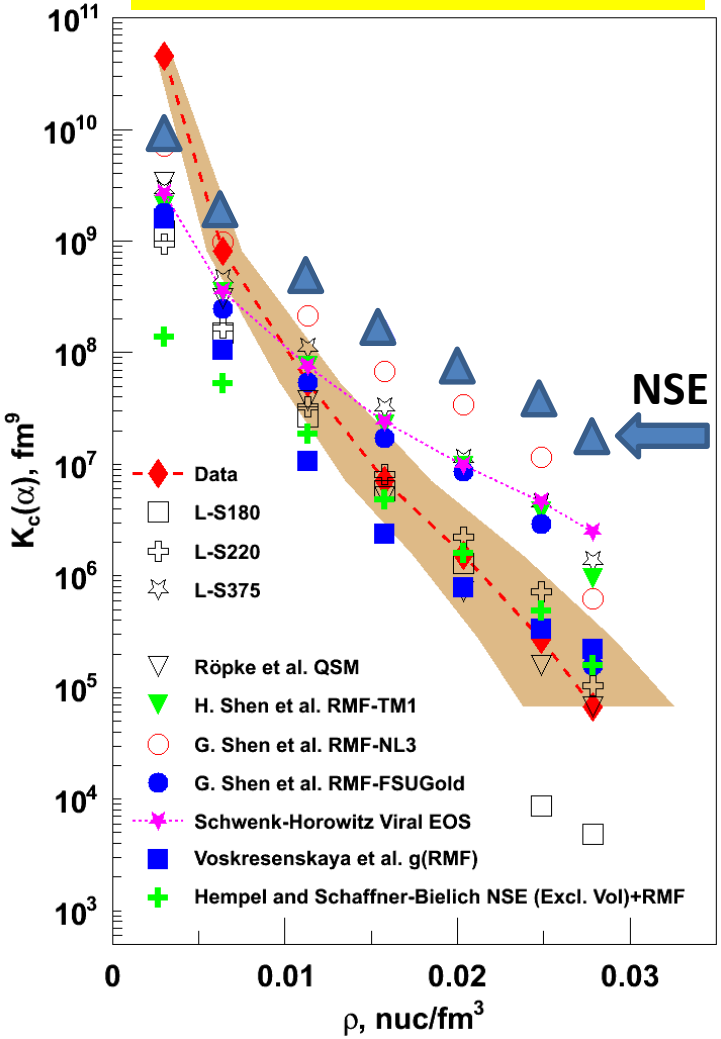

CYCLOTRON INSTITUTE
Texas A&M University

Comparison With EOS Models

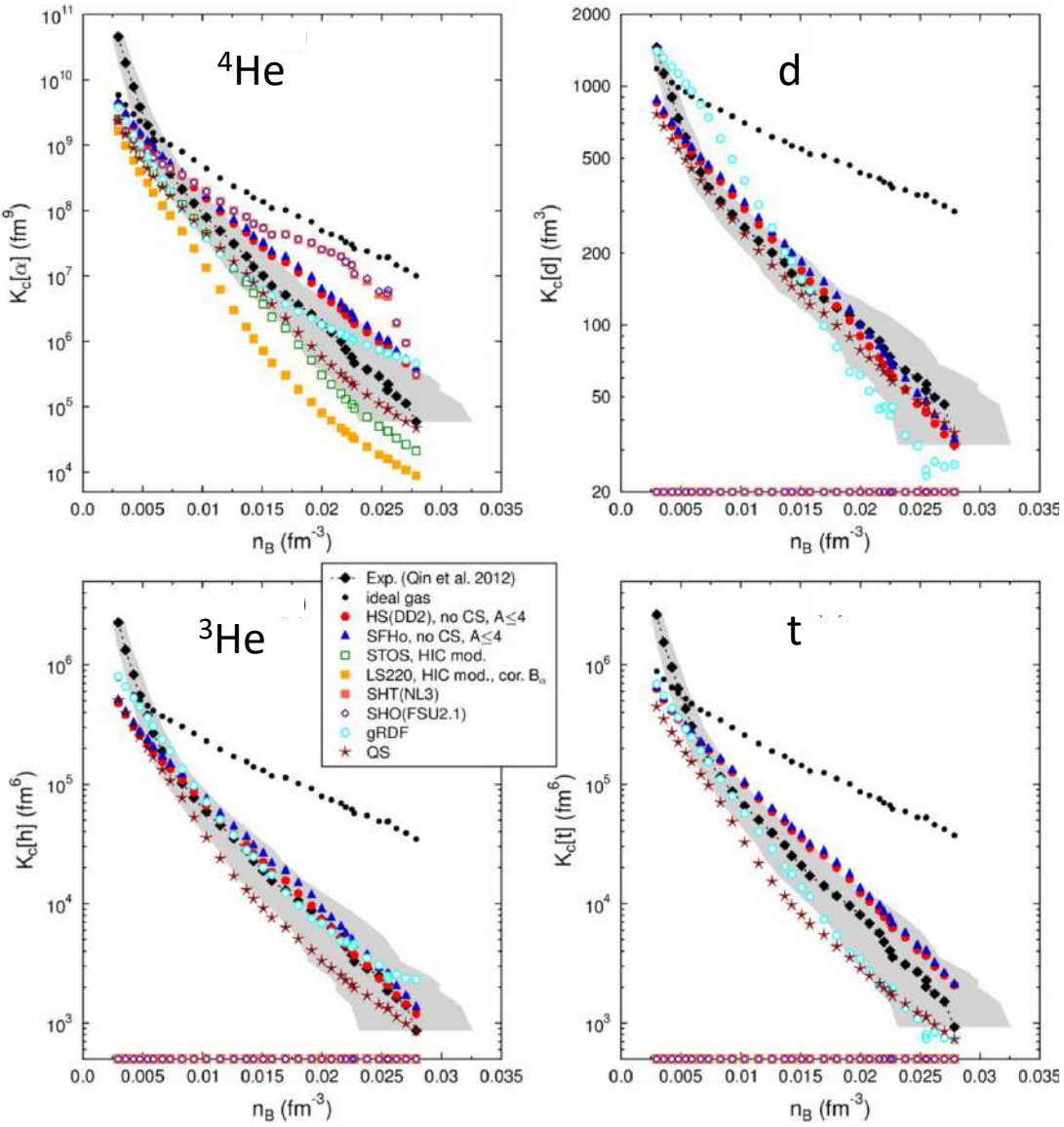

- Two groups of calculations
  - n, p, a calculations which predict $K_{eq}(a)$, but cannot predict other species.
  - Models with n, p, d, t, ^{3}He, a
- Low densities
  - All $K_{eq}(a)$ converge to ideal gas
  - They are below experimental data which result from the very late stages of the reaction
- Models that treat all light particles are generally within error bars

M. Hempel et al.
Phys. Rev. C **91**, 045805 (2015).

SYMMETRY ENERGY LOW DENSITY LIMIT

At Low Density The Symmetry Energy is Determined by Cluster Formation. Analysis of Cluster Yield Ratios For Different N/Z Systems (ISOSCALING) Allows Determination of The Symmetry Free Energy. Employment of Entropies Calculated with the QSM Model of Roepke, Typel et al (shown to be appropriate by other measured quantities) Allows Extraction of The LOW Density Symmetry Energy $F_{sym} + T \cdot S_{sym} = E_{sym}$

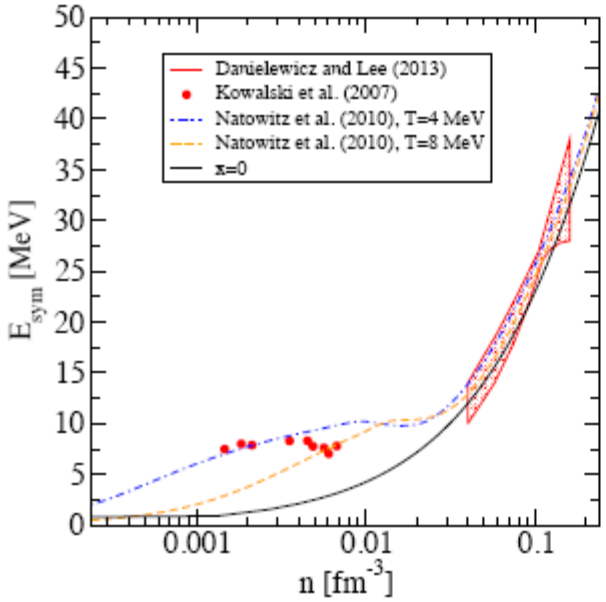

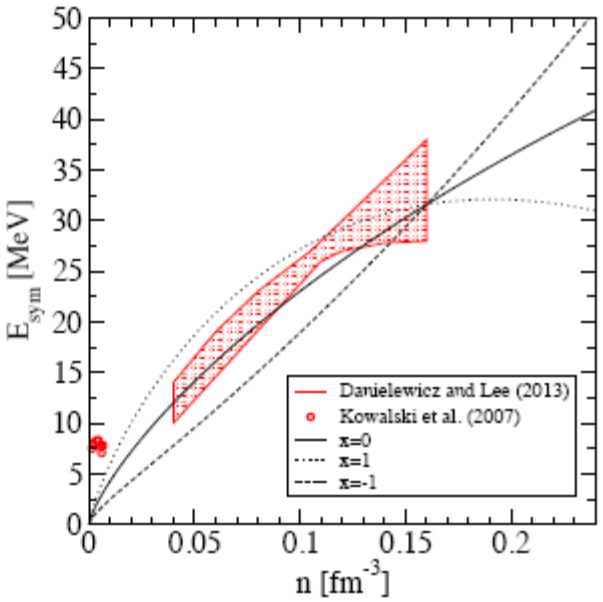

The equation of state and symmetry energy of low density nuclear matter
K. Hagel, G. Roepke and J. Natowitz , EPJA, **50**, 39 (2014)
See also **S. Typel *et al*., Phys. Rev. C 81, 015803 (2010).**
J.B. Natowitz et al., Phys.Rev.Lett.104:202501 (2010).

NOTE CHEMICAL EQUILIBRIUM ASSUMPTIONS FOR FIREBALL

In Medium Effects-Density Dependent Binding Energies – Mott Points

- From Albergo, recall that $K_c(A,Z) = \mathrm{C(T)}e^{\left(\frac{B(A,Z)}{T}\right)}$
- Invert to calculate binding energies
- Entropy mixing term $\Delta F = T\left(Zln\left(\frac{Z}{A}\right) + Nln\left(\frac{N}{A}\right)\right)$

$$ln[K_c/C(T)] = \frac{B}{T} - Zln\left(\frac{Z}{A}\right) - Nln(\frac{N}{A})$$

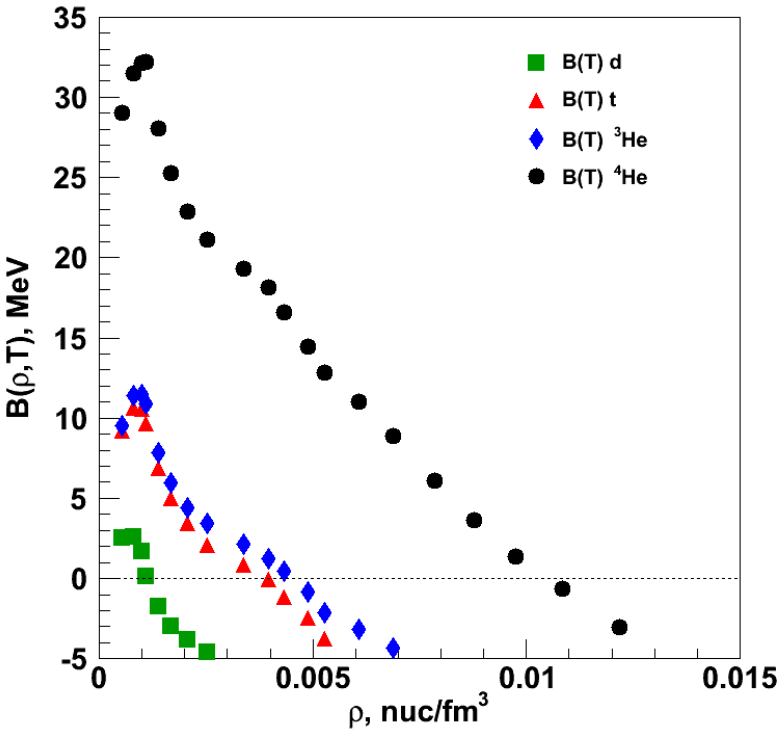

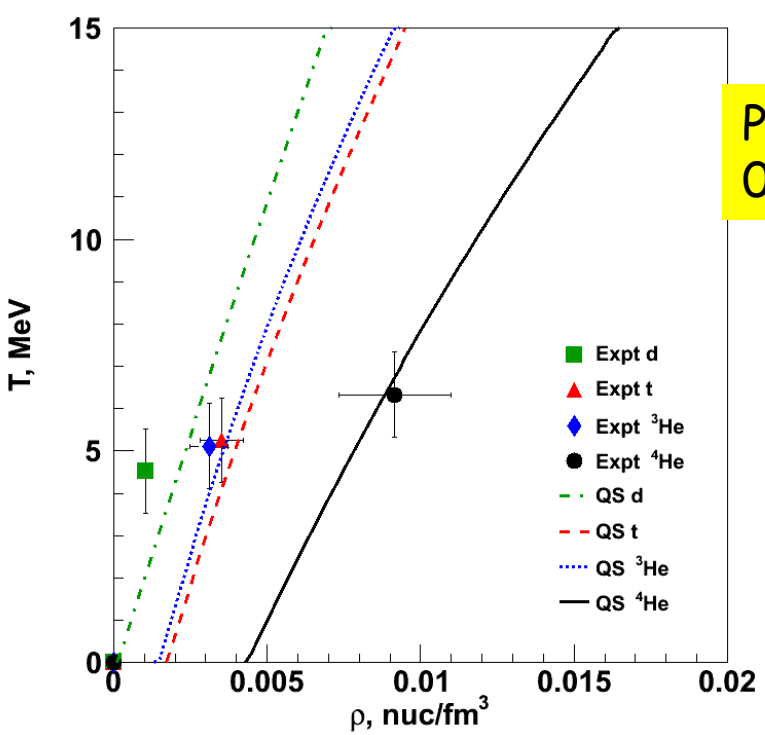

PRL **108** (2012) 062702

Available online at www.sciencedirect.com
ScienceDirect
Nuclear Physics A 776 (2006) 55–79

Cluster formation and the virial equation of state of low-density nuclear matter

C.J. Horowitz, A. Schwenk *

Nuclear Theory Center and Department of Physics, Indiana University, Bloomington, IN 47408, USA

Received 22 November 2005; received in revised form 1 February 2006; accepted 30 May 2006
Available online 7 July 2006

Can we explore lower Rho, Lower T Region ?

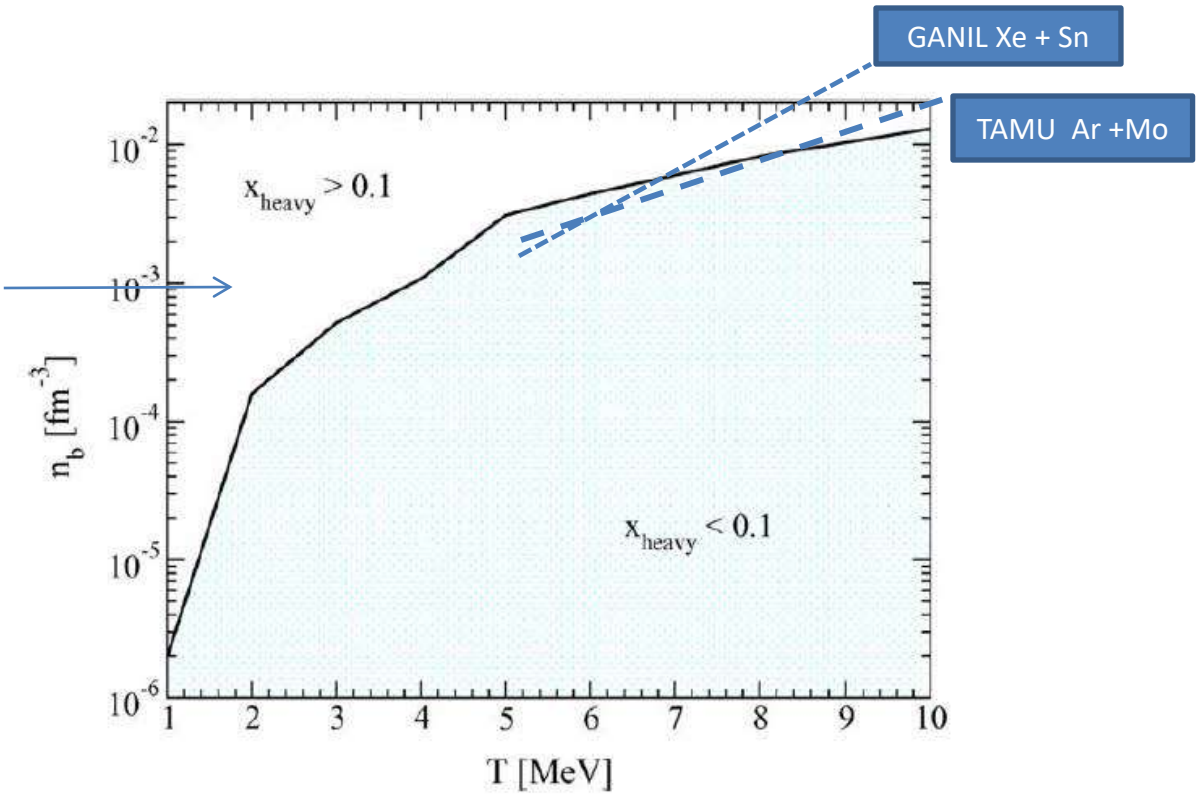

Fig. 9. (Color online.) The threshold baryon density n_b above which the Shen equation of state [27] predicts a heavy nuclei mass fraction larger than 10%. This figure is for $Y_p = 1/2$.

Clustering in the Skins of Leptodermous Systems Should Be A Universal Property

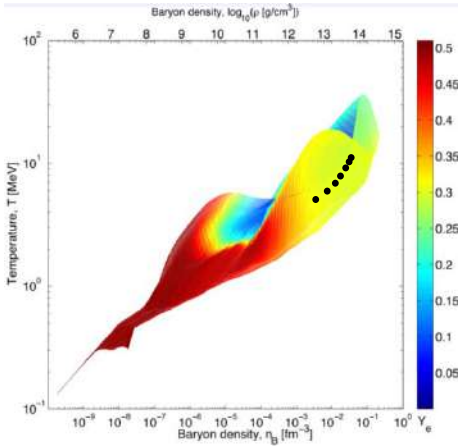

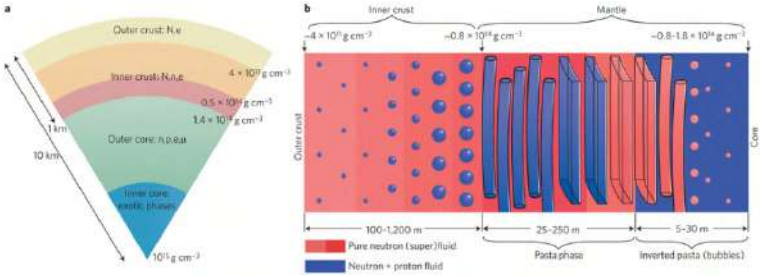

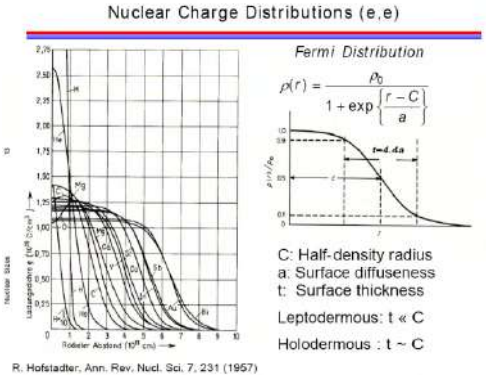

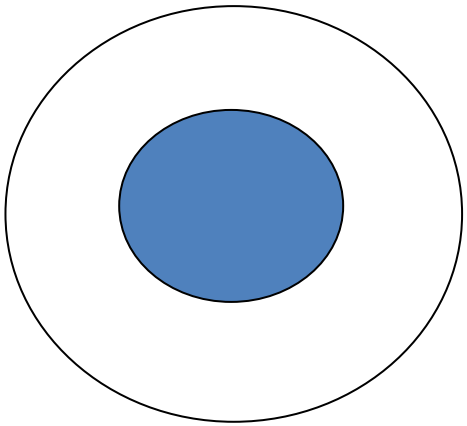

Core Collapse Supernova
r ~ 100 km

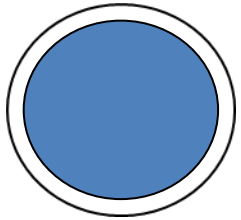

Neutron Star
r ~ 10 km

Nucleus
r ~ 10^{-17} km

LCP Emission in Spontaneous and Thermal Neutron Induced Fission is a Well Studied Process

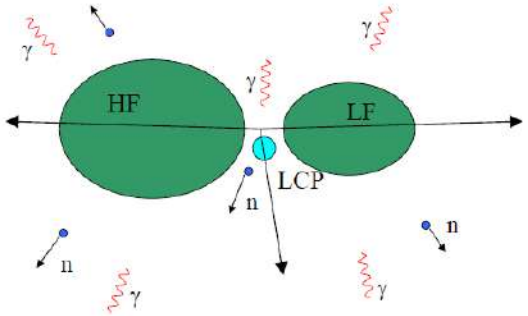

While the probability of ternary fission relative to binary fission is very small (~1/500)

Ternary Fission is a Unique Tool to Study the Energetics and Dynamics of the Fission Process <u>at Scission</u>

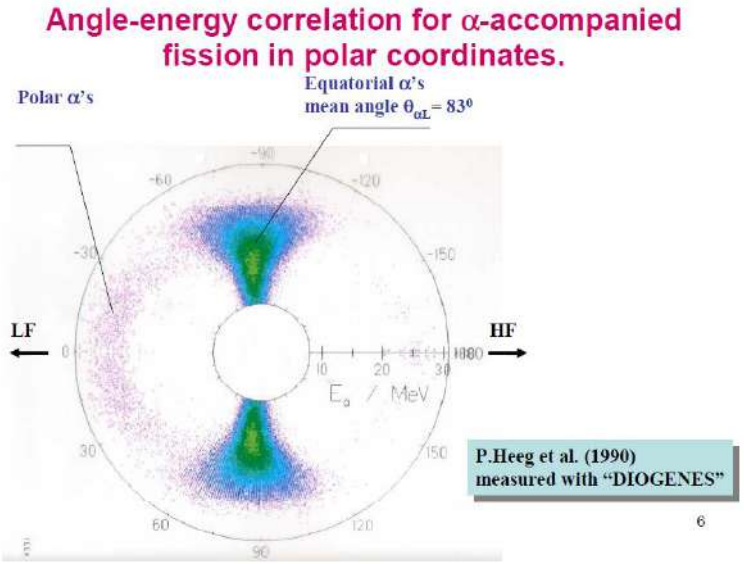

^{252}Cf - Thesis T U Darmstadt

- LCP's are emitted nearly perpendicular to the fission axis
- > 90% of all ternary particles are α-particles
- Yields of heavier particles drastically decreases with the increase of LCP mass
- The energy distribution of LCP has nearly Gaussian shape with $\langle E_\alpha \rangle \approx 15$ MeV
- The emission of LCP slightly changes energy and mass distributions of fission fragments as well as other parameters, e.g. $\bar{\nu}$, M_γ etc.

Question- Can Ternary Fission Be Used to Probe the Equation of State of Low Density Nuclear Matter ?

ELSEVIER

Nuclear Physics A 652 (1999) 371–387

NUCLEAR PHYSICS A

www.elsevier.nl/locate/npe

Ternary fission yields of $^{241}Pu(n_{th},f)$

U. Köster [a,1], H.Faust [b], G. Fioni [c], T. Friedrichs [b,d], M. Groß [e], S. Oberstedt [b]

[a] *Technische Universität München, Physik-Department, 85748 Garching, Bavaria, Germany*
[b] *Institut Laue Langevin, 38042 Grenoble, France*
[c] *CEA Saclay, DSM/DAPNIA/SPHN, 91191 Gif-sur-Yvette, France*
[d] *Technische Universität Braunschweig, Institut für Metallphysik und Nukleare Festkörperphysik, 38106 Braunschweig, Germany*
[e] *Ludwig-Maximilians-Universität, Sektion für Physik, 85748 Garching, Bavaria, Germany*

Received 8 February 1999; revised 18 February 1999; accepted 23 February 1999

Abstract

Ternary events in the thermal neutron induced fission of $^{241}Pu(n,f)$ were studied with the recoil separator LOHENGRIN at the high-flux reactor of the Institut Laue Langevin in Grenoble. Yields and energy distributions could be determined for most isotopes of the elements hydrogen to oxygen. Also several heavier nuclei up to ^{30}Mg could be observed. Yields were measured for 42 isotopes, for further 17 isotopes upper limits could be deduced. For the first time the halo nuclei ^{11}Li, ^{14}Be and ^{19}C were found in neutron induced fission with yields of some 10^{-10} per fission.

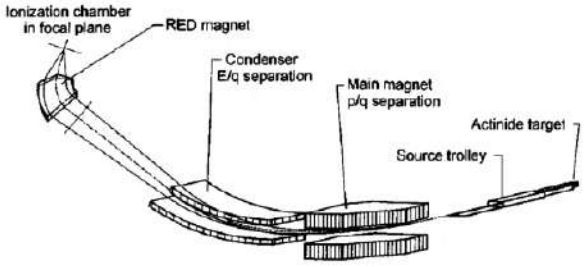

Fig. 1. Arrangement of the recoil separator LOHENGRIN.

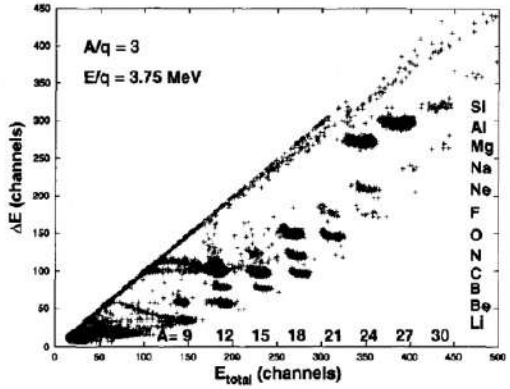

Fig. 3. ΔE–E scatter plot with separator setting $A/q = 3$ and $E/q = 3.75$ MeV. The measurement time for this spectrum was 6.1 h. The horizontal scale is proportional to the particle energy (and due to a fixed A/E ratio also to the mass), whereas the vertical scale is roughly proportional to the nuclear charge Z. Scattered binary particles create background close to the diagonal in the upper part of the spectrum. Background in the lower part is due to pile-up (from abundant ^{3}H and ^{6}He) and particles scattered in the entrance window of the ionization chamber (tails going to the top and left which can be seen at ^{6}He, ^{9}Li and ^{12}C). One channel corresponds approximately to 75 keV.

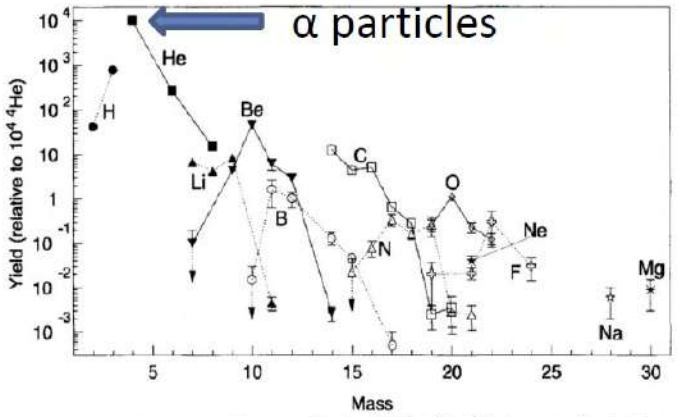

Fig. 7. Measured yields of ternary particles normalized to 10^4 for ^{4}He. The isotopes of each element are connected by a line, dashed for odd Z and solid for even Z. Upper limits are marked with an arrow. Some upper limits have been omitted for sake of clarity.

Nucleation and cluster formation in low-density nucleonic matter: A mechanism for ternary fission

S. Wuenschel[1], H. Zheng[1], K. Hagel[1], B. Meyer[2], M. Barbui[1], E.J. Kim[1,3], G. Röpke[4] and J. B. Natowitz[1]
[1] *Cyclotron Institute, Texas A&M University, College Station, TX 77843, USA;*
[2] *Department of Physics and Astronomy, Clemson University, Clemson, SC 29634, USA;*
[3] *Division of Science Education, Chonbuk National University, Jeonju 561-756, Korea;*
[4] *University of Rostock, FB Physik, Rostock, Germany.*

Ternary fission yields in the reaction ^{241}Pu(n$_{th}$, f) are calculated using a new model which assumes a nucleation-time moderated chemical equilibrium in the low density matter which constitutes the neck region of the scissioning system. The temperature, density, proton fraction and fission time required to fit the experimental data are derived and discussed. A reasonably good fit to the experimental data is obtained. This model provides a natural explanation for the observed yields of heavier isotopes relative to those of the lighter isotopes, the observation of low proton yields relative to ^{2}H and ^{3}H yields and the non-observation of ^{3}He, all features which are shared by similar thermal neutron induced and spontaneous fissioning systems.

Phys. Rev. C **90** 011601(R)
Published 8 July 2014

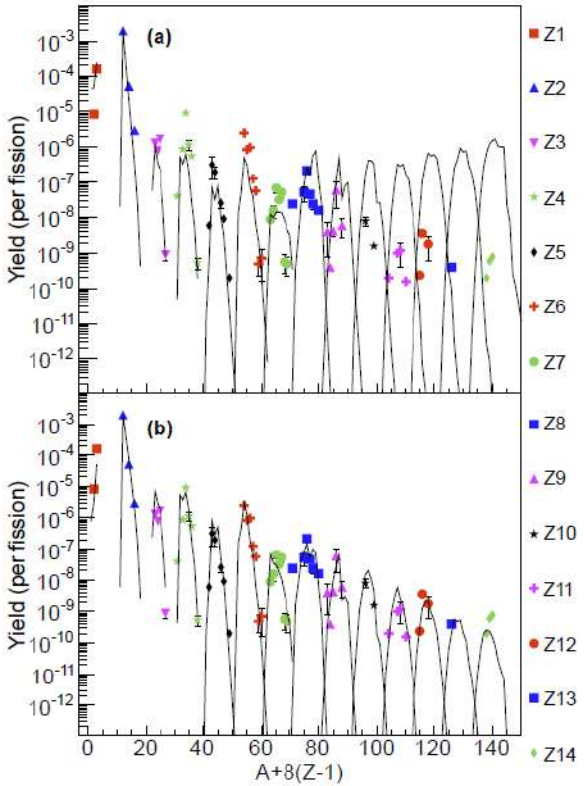

Figure 2: (Color online) Yield per fission as a function of mass(A) and charge(Z) of products. Solid points represent $^{241}Pu(n_{th}, f)$ experimental yields from Koester *et al* [9]. Lines are theoretical predictions from NSE calculation [7]. NSE parameters are $T = 1.4MeV$, $\rho = 4 \times 10^{-4} fm^{-3}$, and $Y_p = 0.34$. a) NSE calculation only. M^2 fit metric = 4.28. b) NSE calculation with nucleation. Nucleation parameters are time = $6400 fm/c$ and $A_c = 5.4$. Fit metric = 1.18.

CYCLOTRON INSTITUTE
Texas A&M University

Available online at www.sciencedirect.com
ScienceDirect
Nuclear Physics A 776 (2006) 55–79
NUCLEAR PHYSICS A

Cluster formation and the virial equation of state of low-density nuclear matter

C.J. Horowitz, A. Schwenk *

Nuclear Theory Center and Department of Physics, Indiana University, Bloomington, IN 47408, USA

Received 22 November 2005; received in revised form 1 February 2006; accepted 30 May 2006
Available online 7 July 2006

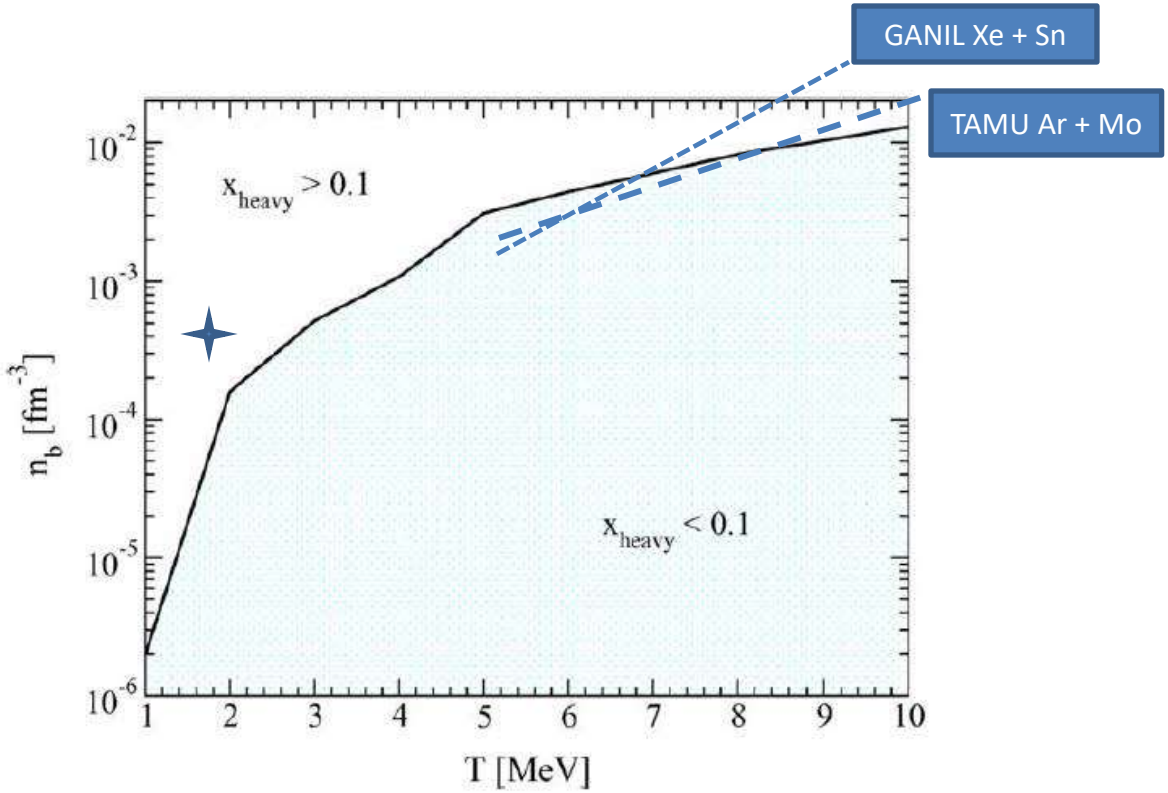

Fig. 9. (Color online.) The threshold baryon density n_b above which the Shen equation of state [27] predicts a heavy nuclei mass fraction larger than 10%. This figure is for $Y_p = 1/2$.

Experimental Determination of $K_{EQ}(\alpha)$

Ternary yields from the relevant literature

TABLE I. Adopted values of neutron, proton, and ^{4}He yields [21,22,35–44]. References are the primary sources. Measurements and systematics of other data for adjacent isotopes were also employed in establishing these values. Uncertainties are 1σ.

Particle	Total yield/fission	Equatorial scission emission	Adopted yield
n	2.96 ± 0.005	0.107 ± 0.015	0.107 ± 0.015
p	$4.08 \times 10^{-5} \pm 0.41$	$3.49 \times 10^{-5} \pm 0.35$	$3.49 \times 10^{-5} \pm 0.35$
^{4}He	$2.015 \times 10^{-3} \pm 0.20$	$2.00 \times 10^{-3} \pm 0.20$	$1.66 \times 10^{-3} \pm 0.17$

(equatorial emission only)
(^{5}He decay contribution removed)

Coalescence Model Volume Calculation - (Mekjian Model) - 2937 fm^3

Particle Densities	K_α^{EXPT}
Rho n 3.64E-05	$3.02(\pm 1.07) \times 10^{18}$ fm^9
Rho p 1.19E-08	
Rho α 5.65E-07	

Evidence of a medium Effect?

NSE K_α	**4.86E+18**
PAIS K_α (FSU-GOLD,0.85)	**2.99E+18**
PAIS K_α (FSU-GOLD,0.92)	**3.75E+18**

H. Pais, F. Gulminelli, C. Providencia, and G. Röpke, Phys. Rev. C **97**, 045805 (2018).
H. Pais, R. Bougault, F. Gulminelli, C. Providencia, E. Bonnet, B. Borderie *et al.*, Phys. Rev. Lett. **125**, 012701 (2020).

Isotopic equilibrium constants for very low-density and low-temperature nuclear matter

J. B. Natowitz,[1] H. Pais,[2] G. Röpke,[3] J. Gauthier,[1] K. Hagel,[1] M. Barbui,[1] and R. Wada[1]
[1]*Cyclotron Institute, Texas A&M University, College Station, Texas 77843, USA*
[2]*Department of Physics, University of Coimbra, 3004-516 Coimbra, Portugal*
[3]*University of Rostock, FB Physik, 18059 Rostock, Germany*

(Received 14 September 2020; accepted 24 November 2020; published 23 December 2020)

Yields of equatorially emitted light isotopes, $1 \leqslant Z \leqslant 14$, observed in ternary fission in the reaction ^{241}Pu $(n_{\rm th}, {\rm f})$ are employed to determine apparent chemical equilibrium constants for low-temperature and low-density nuclear matter. The degree of equilibration and the role of medium modifications are probed through a comparison of experimentally derived reaction quotients with equilibrium constants calculated using a relativistic mean-field model employing a universal medium modification correction for the attractive σ meson coupling. The results of these comparisons indicate that equilibrium is achieved for the lighter ternary fission isotopes. For the heavier isotopes experimental reaction quotients are well below calculated equilibrium constants. This is attributed to a dynamical limitation reflecting insufficient time for full equilibrium to develop. The role of medium effects leading to yield reductions is discussed, as is the apparent enhancement of yields for ^{8}He and other very neutron-rich exotic nuclei.

Pais Calculation(0.92) Includes
Koster Reported Isotopes
59
AND
31 Particle Unstable States
> 268 Gamma decaying States

BNL ENSDFENSDF Evaluated Nuclear Structure Data File, https://www.nndc.bnl.gov/

H. Pais, F. Gulminelli, C. Providencia, and G. Röpke, C **97**, 045805 (2018).
H. Pais, R. Bougault, F. Gulminelli, C. Providencia, I
B. Borderie *et al.*, Phys. Rev. Lett. **125**, 012701 (202

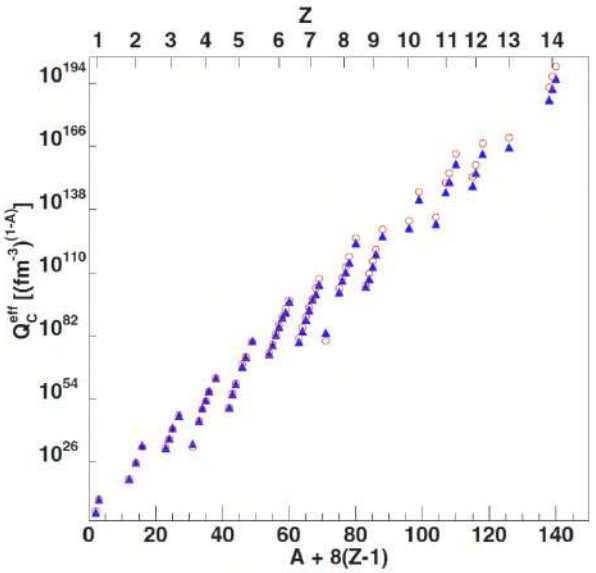

FIG. 1. $Q_c^{\rm eff}$ values vs $A + 8(Z - 1)$. Triangles are experimental results. Open circles are theoretical results for $K_c^{\rm eff}$ with $T = 1.4$ MeV, $Y_p = 0.34$, $\rho = 2.56 \times 10^{-4}$ fm^{-3} and coupling constant $x_{i,\sigma} = 0.92$. An auxiliary Z scale is shown at the top of the figure.

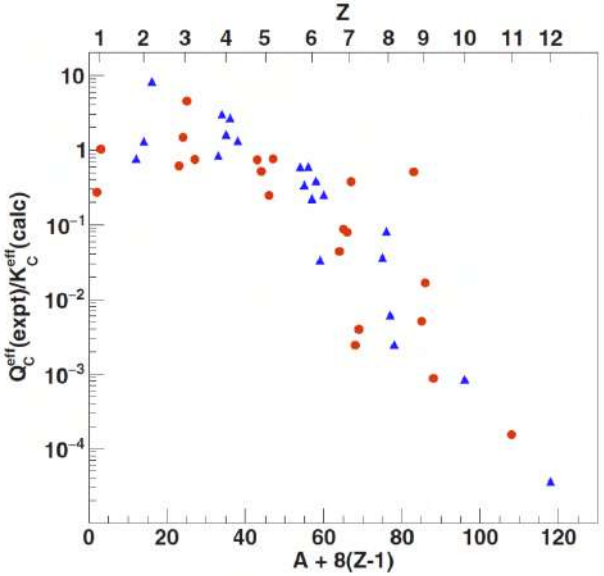

FIG. 2. Ratio $Q_c^{\rm eff}$ (experiment)/$Q_c^{\rm eff}$ (theory) vs $A + 8(Z - 1)$. Solid red circles represent results for odd-Z isotopes. Solid blue triangles represent results for even-Z isotopes. An auxiliary Z scale is shown at the top of the figure. All isotopes in the Koester data table are considered. Isotopes for which only upper limits are reported are excluded from this plot. See text.

CYCLOTRON INSTITUTE
Texas A&M University

A Non-equilibrium Information Entropy Approach to Ternary Fission of Actinides

G. Röpke[1],* J. B. Natowitz[2],† and H. Pais[3‡]
[1] *Institut für Physik, Universität Rostock, D-18051 Rostock, Germany.*
[2] *Cyclotron Institute, Texas A&M University, College Station, Texas 77843, USA.*
[3] *CFisUC, Department of Physics, University of Coimbra, 3004-516 Coimbra, Portugal.*
(Dated: May 3, 2021)

A somewhat different approach-Shannon Information Entropy. No a priori Assumption of Equilibrium.

Using a Virial Equation of State including continuum corrections the evolving distribution is characterized by time dependent Lagrange Multipliers,λ_T,λ_p,λ_n.

In the limit of thermodynamic equilibrium, the information entropy can be identified with the thermodynamic entropy, and the Lagrange Multipliers, ; can be identified with the thermodynamic variables T,μ_p,μ_n.

isotope	$R^{\rm vir}_{A,Z}(1.3)$	^{233}U($n_{\rm th}$,f)	^{235}U($n_{\rm th}$,f)	^{239}Pu($n_{\rm th}$,f)	^{241}Pu($n_{\rm th}$,f)	^{248}Cm(sf)	^{252}Cf(sf)
λ_T [MeV]	-	1.24177	1.21899	1.3097	1.1900	1.23234	1.25052
λ_n [MeV]	-	-3.52615	-3.2672	-3.46688	-3.02055	-2.92719	-3.1107
λ_p [MeV]	-	-15.8182	-16.458	-16.2212	-16.6619	-16.7798	-16.7538
^{1}n	-	560012	1.409e6	722940	1.8579e6	1.606e6	1.647e6
^{1}H	-	28.131	28.16	42.638	19.52	21.079	30.096
^{2}H$^{\rm obs}$	-	41	50	69	42	50	63
^{2}H	0.973	40.986	49.76	68.632	41.563	49.533	61.579
^{3}H$^{\rm obs}$	-	460	720	720	786	922	950
^{3}H	0.998	457.27	715.29	714.79	780.39	913.76	943.12
^{4}H	0.0876	2.7772	4.97	5.627	6.057	8.742	8.219
^{3}He	0.997	0.0124	0.0076	0.0235	0.00131	0.00645	0.00933
^{4}He$^{\rm obs}$	-	10000	10000	10000	10000	10000	10000
^{4}He	1	8858.46	8706.1	8615.7	8556.9	8313.98	8454.0
^{5}He	0.689	1130.75	1289.04	1374.7	1439.0	1680.75	1540.9
^{6}He$^{\rm obs}$	-	137	191	192	260	354	270
^{6}He	0.933	115.89	158.98	159.01	211.68	276.96	222.4
^{7}He	0.876	21.262	33.997	35.983	51.742	80.634	58.16
$Y^{\rm obs}_{^6{\rm He}}/Y^{\rm final,vir}_{^6{\rm He}}$	-	0.9989	0.9897	0.9846	0.9869	0.9899	0.9622
^{8}He$^{\rm obs}$	-	3.6	8.2	8.8	15	24	25
^{8}He	0.971	3.4725	6.764	6.4095	12.481	21.280	13.32
^{9}He	0.255	0.047077	0.105	0.111	0.219	0.455	0.258
$Y^{\rm obs}_{^8{\rm He}}/Y^{\rm final,vir}_{^8{\rm He}}$	-	1.0229	1.1936	1.3496	1.1811	1.1042	1.8409
^{8}Be	1.07	5.7727	2.594	5.147	2.188	2.819	2.544

TABLE I: Lagrange parameters λ_i, observed yields $Y^{\rm obs}_{A,Z}$ (rows denoted with $^{A}Z^{\rm obs}$) [10, 13, 40], and primary yields $Y^{\rm rel,vir}_{A,Z}$ (rows denoted with ^{A}Z) for H and He nuclei from ternary fission of ^{233}U($n_{\rm th}$,f), ^{235}U($n_{\rm th}$,f), ^{239}Pu($n_{\rm th}$,f), ^{241}Pu($n_{\rm th}$,f), ^{248}Cm(sf), and ^{252}Cf(sf). The prefactor $R^{\rm vir}_{A,Z}(\lambda_T)$ at $\lambda_T = 1.3$ MeV, which represents the intrinsic partition function, is also given. In addition, two rows show the ratio of the observed yields compared to the final yields $Y^{\rm final,vir}_{^6{\rm He}} = Y^{\rm rel,vir}_{^6{\rm He}} + Y^{\rm rel,vir}_{^7{\rm He}}$ and $Y^{\rm final,vir}_{^8{\rm He}} = Y^{\rm rel,vir}_{^8{\rm He}} + Y^{\rm rel,vir}_{^9{\rm He}}$. Note that *vir* stands for virial approximation. For details see the Supplementary Material [41].

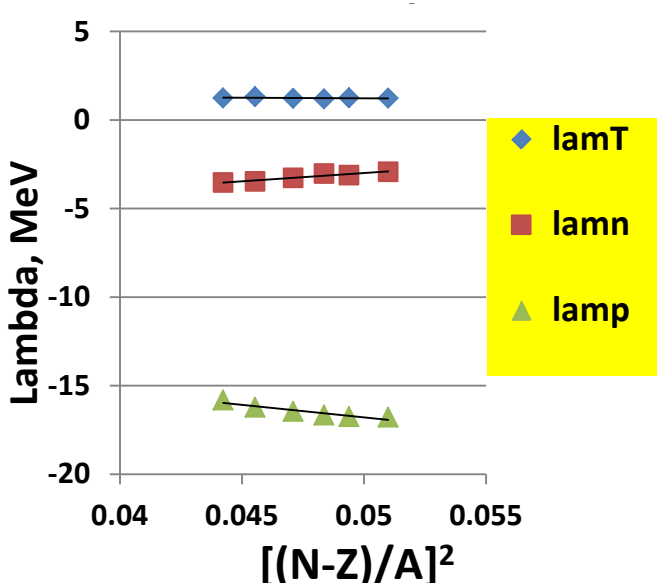

CYCLOTRON INSTITUTE
Texas A&M University

Comparison of Observed and Calculated Yields

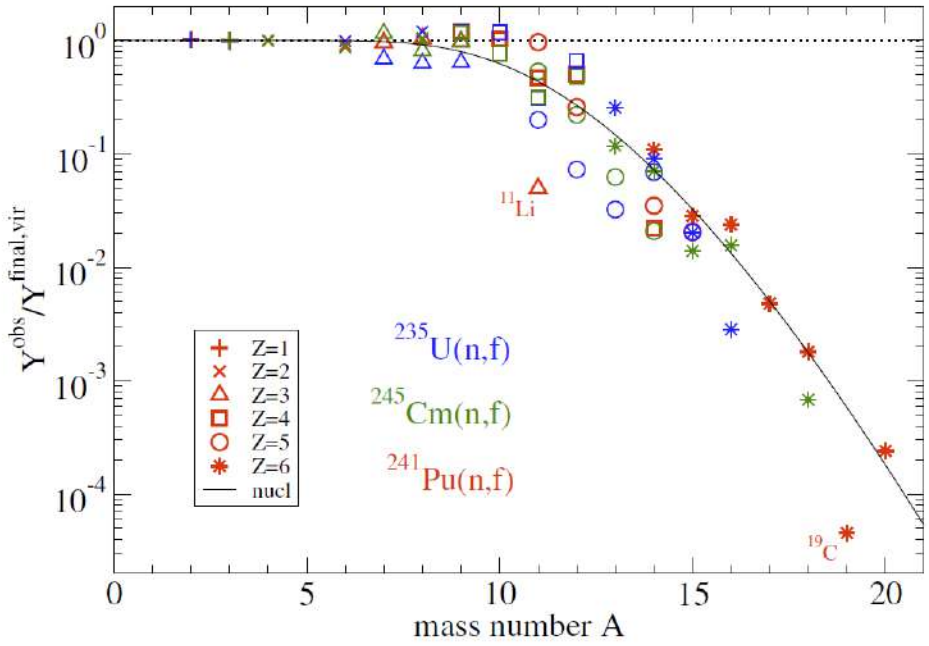

FIG. 1: Ternary fission of ^{235}U($n_{\rm th}$,f) (blue), ^{245}Cm($n_{\rm th}$,f) (green), and ^{241}Pu($n_{\rm th}$,f) (red): Ratio $Y^{\rm obs}_{A,Z}/Y^{\rm final,vir}_{A,Z}$ as function of the mass number A. Isotopes with $Z \leq 6$ are shown. Black full line: Fit of nucleation kinetics (6) to the data of ^{241}Pu($n_{\rm th}$,f).

Question- Can Ternary Fission Be Used to Probe the Equation of State of Low Density Nuclear Matter ?

The Answer is Yes

For Equatorially Emitted Isotopes With A< 10 Isotopes
Chemical Equilibrium Appears to be Achieved. A Virial EOS successfully reproduces the observed yields.

For Heavier Isotopes the Data Indicate That There is Insufficient Time for Equilibrium to be Reached

Data of Higher Accuracy Would Allow Careful Evaluation of In-Medium Effects

Explorations of Equatorial LCP and Fragment Emission in Mid=Peripheral Collisions Might Allow Investigation of a Broader Range of ρ and T.

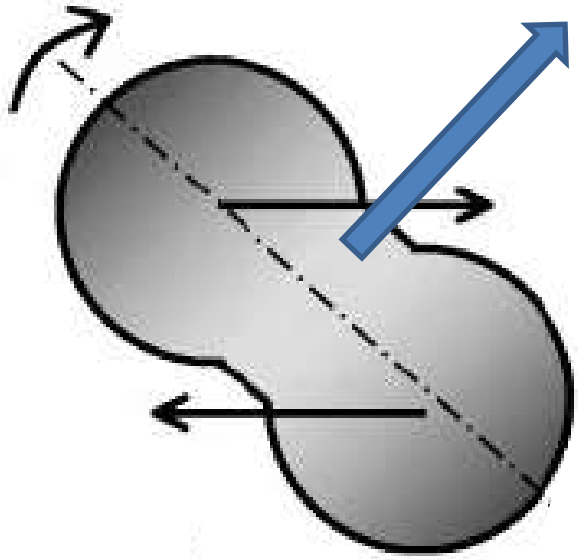

Collaborators

K. Hagel, R. Wada, S. Kowalski, L. Qin, S. Wuenschel, M. Barbui, J. Gauthier, K. Schmidt, E. J. X. Cao, Kim,G. Röpke, M. Hempel, S. Typel, H.Pais, G. Giuliani, S. Shlomo, A. Bonasera, Z. Chen, M. Huang, J. Wang, H. Zheng, M. R. D. Rodrigues, D. Fabris, M. Lunardon, S. Moretto, G. Nebbia, S. Pesente, V. Rizzi, G. Viesti, M. Cinausero, G. Prete, T. Keutgen, Y. El Masri, Z. Majka, Y. G. Ma and J. B. Natowitz,

Texas A&M University, College Station, Texas
INFN Laboratori Nazionali di Legnaro, Legnaro, Italy
INFN Dipartimento di Fisica, Padova, Italy
Jagellonian University, Krakow, Poland
Silesian University, Katowice, Poland
Universität Darmstadt, Darmstadt, Germany
University of Rostock, Rostock, Germany
Basel University, Basel, Switzerland
UCL, Louvain-la-Neuve, Belgium
Shanghai Institute of Nuclear and Applied Physics, Shanghai, China
University of Coimbra, Coimbra, Portugal

CYCLOTRON INSTITUTE
Texas A&M University